Article

Discovery Medicine 2025; 37(201): 2192–2204
https://doi.org/10.24976/Discov.Med.202537201.186

Right-Sided Stellate Ganglion Block Ameliorates Insomnia-Induced Neuronal Damage and Cognitive Impairment by Suppressing Ferroptosis via NRF2/GPX4 Pathway

Meiyue Liu[1,†], Xi Ouyang[1,†], Yun Shao[2], Qing Zhang[1,*]

[1]Department of Anesthesiology, Zhabei Central Hospital, 200072 Shanghai, China
[2]Department of Anesthesiology, Fudan University Affiliated Stomatological Hospital (Shanghai Stomatological Hospital), 200001 Shanghai, China
*Correspondence: zhangqing9836@126.com (Qing Zhang)
[†]These authors contributed equally.
Submitted: 1 July 2025 Revised: 15 August 2025 Accepted: 25 August 2025 Published: 20 October 2025

Background: Innovative therapies are urgently required for treating insomnia, a prevalent neurological disorder associated with multisystem comorbidities. This study aims to explore the neuroprotective potential of right-sided stellate ganglion block (SGB) against insomnia-induced neuronal damage and cognitive dysfunction, focusing on ferroptosis modulation through the nuclear factor-erythroid 2-related factor 2 (NRF2)/glutathione peroxidase 4 (GPX4) pathway.

Methods: A rat model of insomnia was established through para-chlorophenylalanine (PCPA) induction. Interventions tested in this study included right-sided SGB (1% lidocaine), ferroptosis modulators (RAS-Selective Lethal 3 (RSL3), ferrostatin-1 (Fer-1)), and an NRF2 inhibitor (ML385). Cognitive performance of the rats was evaluated using the Morris water maze. Neuronal integrity was examined through histopathologic assessments (HE/Nissl staining), evaluation of synaptic markers (synuclein (SYN)/postsynaptic density protein 95 (PSD-95) immunohistochemistry), and detection of glial activation (ionized calcium-binding adaptor molecule 1 (Iba-1)/glial fibrillary acidic protein (GFAP) immunofluorescence). Neurotransmitters (serotonin (5-HT)/γ-aminobutyric acid (GABA)/dopamine (DA)/noradrenaline (NE)), brain redox status (malondialdehyde (MDA)/glutathione (GSH)/reactive oxygen species (ROS)), and neuroinflammation (tumor necrosis factor-α (TNF-α)/interleukin-1β (IL-1β)/interleukin-6 (IL-6)) were assessed by means of ELISA. Western blotting was used to analyze the expression of proteins related to iron metabolism (ferritin heavy chain (FTH1)/ferritin light chain (FTL)/transferrin receptor 1 (TFR1)) and the NRF2/GPX4 pathway.

Results: SGB treatment reversed PCPA-induced cognitive deficits, as evidenced by reduced escape latency and increased target quadrant dwell time ($p < 0.05$). Histologic staining revealed that SGB rescued synaptic density and attenuated neuronal loss ($p < 0.05$). Mechanistically, SGB suppressed ferroptosis by normalizing iron homeostasis, suppressing lipid peroxidation, and inhibiting ROS overproduction, while mitigating neuroinflammation (both $p < 0.05$). Treatment with ML385 negated SGB's benefits, indicating that these effects can be mediated by NRF2/GPX4 pathway activation, whereas Fer-1 restored the neuroprotective effects of SGB ($p < 0.05$).

Conclusion: Right-sided SGB alleviates cognitive deficits and neuronal injury in insomniac rats by activating the NRF2/GPX4 pathway to inhibit ferroptosis and neuroinflammation, offering a novel neuromodulatory therapy for insomnia-related neurodegeneration.

Keywords: insomnia; right-sided stellate ganglion block; ferroptosis; NRF2/GPX4 signaling pathway; cognitive impairment

Introduction

Insomnia, a neurological disorder impacting over 30% of adults worldwide [1], is characterized by difficulty falling or staying asleep [2]. It has a multifactorial etiology and is associated with substantial personal and societal burdens [3]. Beyond its severe impact on sleep quality, accumulating evidence links insomnia to a range of negative health consequences, including cognitive impairments, mood disorders, weakened immune function, gastric ulcers, diabetes, and an increased risk of cardiovascular diseases [4–6]. Current treatments for insomnia, predominantly cognitive-behavioral therapies and pharmacological interventions, are limited by suboptimal efficacy, low patient adherence, and adverse side effects [7], underscoring the need to discover or develop novel and effective therapeutic approaches.

The stellate ganglion is a critical hub of the sympathetic nervous system, located at the junction of the seventh cervical vertebra and the first thoracic vertebra. It plays

an important role in regulating various physiological functions, including circulation, respiration, nociceptive transmission, and neuroendocrine activity [8]. Clinically, stellate ganglion block (SGB), a minimally invasive neuromodulation technique targeting the cervicothoracic sympathetic chain, has become a promising intervention for neuropsychiatric disorders. By blocking sympathetic nerve conduction and reducing sympathetic tone, SGB has demonstrated efficacy in conditions such as post-traumatic stress disorder (PTSD), depression, anxiety, and insomnia [9–11]. However, the potential neuroprotective role of SGB in insomnia-related neurodegeneration remains insufficiently investigated.

Ferroptosis, as a programmed iron-dependent cell death process triggered by iron metabolic imbalance and lipid peroxidation [12], has emerged as a key mediator of sleep deprivation-induced neuronal injury [13]. Central to ferroptosis regulation is the nuclear factor-erythroid 2-related factor 2 (NRF2)/glutathione peroxidase 4 (GPX4) pathway, where NRF2 transcriptionally activates antioxidant genes, such as *GPX4* and glutathione (*GSH*), to maintain redox balance and iron homeostasis [14,15]. Notably, GPX4, the sole selenoprotein that reduces phospholipid hydroperoxides, is critical for ferroptosis resistance [16]. While insomnia is linked to oxidative stress and neuroinflammation [17,18], the interplay between SGB, NRF2/GPX4 signaling, and ferroptosis in this context remains unknown.

On this basis, this study examines the effects of right-sided SGB on neuronal damage and cognitive function (learning/memory) in insomniac rats, and explores the underlying mechanisms involved. We hypothesize that right-sided SGB may improve neuronal damage in insomniac rats by regulating the NRF2/GPX4 pathway, thus enhancing learning and memory function. By thoroughly investigating this mechanism, the study aims to offer new theoretical insights and experimental evidence for the use of right-sided SGB in treating insomnia.

Materials and Methods

Animal Handling and Grouping

Sixty 5-week-old specific pathogen-free Sprague–Dawley rats (each weighing 160–200 g) were obtained from Hunan SJA Laboratory Animal Co., Ltd. (Changsha, China) and acclimatized in an appropriate environment for 3 days.

The rats were randomly assigned to 10 experimental groups (n = 6/group): Control (normal saline), Model (para-chlorophenylalanine [PCPA]), Sham (PCPA + sham SGB), SGB (PCPA + SGB), SGB + NS (PCPA + SGB + normal saline), SGB + RAS-Selective Lethal 3 (RSL3) (PCPA + SGB + RSL3), SGB + ML385 (PCPA + SGB + ML385), SGB + ML385 + Fer-1 (PCPA + SGB + ML385 + ferrostatin-1 [Fer-1]), SGB + sh-NC (PCPA + SGB + adenovirus carrying control shRNA [Ad-shNC]), and SGB + sh-NRF2 (PCPA + SGB + adenovirus carrying sh-NRF2 [Ad-shNRF2]).

All groups except the Control group were intraperitoneally injected with PCPA (300 mg/kg/day, C6506, Merck, Darmstadt, Germany) for 3 consecutive days to induce insomnia. The Control group received equivalent volumes of normal saline [19]. SGB groups were subjected to daily right-sided SGB starting 6 days prior to model induction and continuing throughout the experimental period. The procedure was performed using a professional veterinary anesthesia inhalation system Matrx VIP 3000 (91305430 Isoflurane VIP 3000® - Well-Fill, Midmark, Versailles, OH, USA) equipped with a precision vaporizer and a dedicated rodent circuit. Under 3% isoflurane anesthesia (792632, Merck, Darmstadt, Germany) delivered via the inhalation system, the rats were positioned prone on the surgical table with the neck extended. Using palpation-guided anatomical landmarks, the operator inserted a 1-mL syringe along the right sagittal plane of the seventh cervical vertebra until contacting the transverse process. After 0.5-mm retraction and negative aspiration for blood/cerebrospinal fluid confirmed by plunger withdrawal, 0.3 mL of 1% lidocaine (PHR1034, Merck, Darmstadt, Germany) was administered [20]. The Sham group received saline injections at the same site, while the Control and Model groups received no treatment. Upon waking from anesthesia, the SGB rats exhibited typical Horner's syndrome, including ptosis, narrowed palpebral fissure, and pupil constriction on the blocked side, which are signs of successful SGB. Otherwise, SGB was considered unsuccessful, and those rats without these signs were excluded from subsequent analyses. No exclusions occurred in any of the experimental groups, and all animals initially assigned were included in the final analysis.

ML385 (B8300, APEXBIO, Houston, TX, USA) was intraperitoneally injected at 30 mg/kg 30 minutes prior to each SGB procedure. Post-surgery, RSL3 (5 mg/kg/day, HY-100218A, MedChemExpress, NJ, USA) and Fer-1 (10 mg/kg/day, HY-100579, MedChemExpress, NJ, USA) were intraperitoneally administered for 3 consecutive days. As a negative control, the SGB + NS group received equivalent saline injections. Morris water maze testing commenced after insomnia modeling with PCPA. NRF2 knockdown was achieved by intracerebroventricular injection of Ad-shNRF2 or Ad-shNC (VectorBuilder, Guangzhou, China; serotype Ad5, $\geq 1 \times 10^{10}$ PFU/mL). A 5-µL viral suspension was injected into the right lateral ventricle (coordinates: anteroposterior +0.8 mm, mediolateral +1.2 mm, dorsoventral –2.0 mm relative to bregma) at 0.2 µL/minute. The needle was retained for 1 minute post-injection to prevent reflux. To coincide with peak adenoviral expression, injections were administered 3 days prior to PCPA induction, with knockdown efficiency confirmed by quantitative polymerase chain reaction (qPCR) at day 7 post-injection.

On day 15, the rats were euthanized by intraperitoneal injection of pentobarbital sodium (140 mg/kg, P3761, Merck, Darmstadt, Germany). Brains were immediately extracted and bisected midsagittally. Right hippocampi were sectioned coronally (5 µm) from bregma –2.8 to –3.8 mm, while left hippocampi were immersion-fixed in 4% paraformaldehyde for validation. Every 10th section was kept for hematoxylin and eosin (HE)/Nissl staining. Sections were selected based on: (1) intact dorsoventral hippocampal continuity, (2) uniform staining quality across groups, and (3) blinded assessment using randomly assigned codes. Serum was concurrently collected for biomarker analysis.

Morris Water Maze Experiment

One day before the experiment, all rats were acclimatized to the testing environment with a 5-minute free-swimming session in the Morris water maze. Afterward, the rats were trained over 4 consecutive days to locate a fixed, submerged platform from different quadrants within the pool. On the 5th day, a spatial navigation task was performed by placing the rats in the first quadrant of the pool and recording the time to locate the platform within 60 seconds. On the 6th day, the rats were given a spatial probe test in which the submerged platform was removed and the animals were placed in the first quadrant. The time spent swimming in the quadrant where the platform was previously located was recorded during the 60-second probe.

ELISA

Fresh brain tissues were collected for preparing 10% (w/v) tissue homogenate. The levels of neurotransmitters serotonin (5-HT), γ-aminobutyric acid (GABA), dopamine (DA) and noradrenaline (NE), as well as oxidative stress-related factors such as malondialdehyde (MDA) and GSH, in rat brain tissues were assessed using ELISA kits (5-HT, RK09044, ABclonal, Wuhan, China; GABA, RK09121, ABclonal, Wuhan, China; DA, RK00642, ABclonal, Wuhan, China; NE, RK00694, ABclonal, Wuhan, China; MDA, J23786, Gilead, Wuhan, China; GSH, CB10393-Ra, Coibo, Shanghai, China) according to the manufacturer's instructions. Additionally, rat serum was collected to evaluate the levels of inflammatory cytokines like tumor necrosis factor-α (TNF-α), interleukin-1β (IL-1β), and interleukin-6 (IL-6) using ELISA kits (TNF-α, RK00029, ABclonal, Wuhan, China; IL-1β, RK00009, ABclonal, Wuhan, China; IL-6, RK00020, ABclonal, Wuhan, China) following the manufacturer's instructions. All assays were conducted using a BioTek Synergy H1 microplate reader (Agilent Technologies, USA) at specified wavelengths, in accordance with the manufacturer's protocols.

HE Staining

After fixation in 10% neutral-buffered formalin (MM1521, Maokangbio, Shanghai, China), the rat brain tissues were dehydrated using a graded ethanol series, cleared with xylene (534056, Merck, Darmstadt, Germany), embedded in paraffin, and then cut into sections. Prior to staining, the paraffin-embedded sections were deparaffinized with xylene and rehydrated in a descending ethanol gradient. Staining was performed using a HE staining kit (C0105S, Beyotime, Shanghai, China). Post-staining, the sections were subjected to dehydration using a graded ethanol series, clearing in xylene, and mounting with neutral resin. Histomorphological observation was conducted under a Nikon Eclipse E200 light microscope (Nikon Corporation, Tokyo, Japan), with representative fields captured.

Nissl Staining

The frozen brain tissue sections were stained with Nissl staining solution (C0117, Beyotime, Shanghai, China) for 5 minutes. After mounting, the sections were observed and photographed under an optical microscope (DM8000 M, Leica, Wetzlar, Germany). Nissl bodies were counted using ImageJ software (V1.8.0.112, NIH, Madison, WI, USA).

Immunohistochemistry

Paraffinized rat brain sections were dewaxed for heat-induced antigen retrieval. Endogenous peroxidase activity was eliminated using a 3% hydrogen peroxide solution. The sections were then blocked in phosphate-buffered saline (PBS) containing 10% bovine serum albumin (BSA; V900933, Merck, Darmstadt, Germany) for 1 hour. Subsequently, the sections were incubated overnight at 4 °C with primary antibodies against synapsin (SYN; A6344, 1:100, ABclonal, Wuhan, China) and postsynaptic density protein 95 (PSD-95; A7889PM, 1:500, ABclonal, Wuhan, China). Afterward, the sections were incubated at room temperature for 30 minutes with horseradish peroxidase (HRP)-conjugated secondary antibody (AS014, 1:50, ABclonal, Wuhan, China). Color development was performed using diaminobenzidine (DAB; D5905, Merck, Shanghai, China), followed by counterstaining with hematoxylin. Imaging was captured using a digital ZEISS LSM 900 confocal microscope (Carl Zeiss, Germany).

Immunofluorescence

The frozen sections of rat brain were blocked with PBS solution containing 10% BSA (V900933, Merck, Darmstadt, Germany) for 1 hour. The tissues were then incubated with primary antibodies against ionized calcium-binding adaptor molecule 1 (IBA-1; A19776, 1:100, ABclonal, Wuhan, China) and glial fibrillary acidic protein (GFAP; A19058, 1:100, ABclonal, Wuhan, China) at 4 °C for 24 hours. Afterward, the sections were incubated with fluorescence-labeled secondary antibodies: FITC-conjugated goat anti-rabbit IgG (AP132F, Merck, Darmstadt, Germany) and ABflo® 647-conjugated goat

anti-rabbit IgG (AS060, ABclonal, Wuhan, China) at room temperature for 1 hour. Later, the sections were stained with 4′,6-diamidino-2-phenylindole (DAPI; D1306, Thermo Fisher, Waltham, MA, USA) working solution at room temperature, protected from the light, for 20 minutes. Images were observed and captured using a fluorescence microscope (DM2500, Leica, Wetzlar, Germany). Fluorescence intensity was assessed using ImageJ software.

Iron Content Determination

Brain tissue homogenates were prepared, and ferrous ion contents in the brain tissues were measured using a ferrous ion detection kit (M1217B, Gelatin, Shanghai, China) according to the manufacturer's instructions.

Fluorescent Staining for Reactive Oxygen Species (ROS) Detection

Frozen brain tissue sections were incubated with 10 μM 2′,7′- dichlorodihydrofluorescein diacetate (DCFH-DA; HY-D0940, MedChemExpress, NJ, USA) in the dark for 30 minutes. After removal of unreacted probes, the sections were mounted with an anti-fade mounting medium. The sections were then observed under a fluorescence microscope, and images were captured. Fluorescence intensity was assessed using ImageJ software.

Western Blotting

Total protein was extracted from the rat brain tissues using radioimmunoprecipitation assay (RIPA) buffer (P0013B, Beyotime, Shanghai, China), and protein concentration was determined using the bicinchoninic acid (BCA) protein assay kit (P0009, Beyotime, Shanghai, China). The protein samples were then loaded onto a sodium dodecyl sulfate-polyacrylamide gel electrophoresis (SDS-PAGE) system (NP0007, ThermoFisher, Waltham, MA, USA) for electrophoretic separation. After being transferred to polyvinylidene fluoride (PVDF) membranes (FFP70, Beyotime, Shanghai, China), the proteins were blocked with 5% skim milk and incubated with primary antibodies against NRF2 (ab313825, 68 kDa, 1:1000, Abcam, Cambridge, UK), GPX4 (30388-1-AP, 23 kDa, 1:1000, Proteintech, Wuhan, China), ferritin heavy chain 1 (FTH1; 11682-1-AP, 21 kDa, 1:2000, Proteintech, Wuhan, China), ferritin light chain (FTL; ab69090, 21 kDa, 1:1000, Abcam, Cambridge, UK), transferrin receptor 1 (TFR1; ab214039, 85 kDa, 1:1000, Abcam, Cambridge, UK), and glyceraldehyde-3-phosphate dehydrogenase (GAPDH; A19056, 36 kDa, 1:50,000, ABclonal, Wuhan, China) overnight at 4 °C. Next, the membranes were incubated with HRP-conjugated secondary antibody (ab205718, 1:2000, Abcam, Cambridge, UK) at room temperature for 2 hours. Detection was performed using the BeyoECL Star (P0018S, Beyotime, Shanghai, China) for 30 seconds. Band density was analyzed using ImageJ software.

Statistical Analysis

Statistical analyses were conducted using Prism 9 software (National Institutes of Health, USA), and the results are expressed as mean ± standard deviation (SD). The *t*-test was employed for comparisons between two groups. For datasets involving three or more groups, either one-way or two-way analysis of variance (ANOVA) was applied, followed by Tukey's post-hoc test. A *p*-value of less than 0.05 was deemed statistically significant.

Results

Right-sided SGB Improves Cognitive Impairment in Insomniac Rats

To evaluate the effects of right-sided SGB on cognitive function, an insomnia model was first established in rats using PCPA. ELISA results (Fig. 1A) revealed that, compared to the Control group, rats in the Model group exhibited significantly elevated excitatory neurotransmitters (DA and NE) and reduced inhibitory neurotransmitters (5-HT and GABA), confirming successful model establishment ($p < 0.05$). Interestingly, the SGB-treated rats demonstrated a significant reduction in excitatory neurotransmitter levels and an increase in inhibitory neurotransmitter levels relative to the Sham group ($p < 0.05$). Spatial learning and memory were subsequently assessed using the Morris water maze to determine the cognitive effects of right-sided SGB. On day 5, Model group rats took significantly longer to reach the target platform than those in the Control group. During the probe trial on day 6, they also spent notably less time in the target quadrant containing the original platform. In contrast, the SGB group showed improved performance, reaching the target platform faster than the Sham group on day 5 and spending significantly more time in the original platform quadrant on day 6, as displayed in Fig. 1B,C ($p < 0.05$). These results demonstrate that right-sided SGB alleviates insomnia-induced cognitive dysfunction and exhibits therapeutic potential, with additional neuroprotective benefits.

Right-sided SGB Improves Neuronal Loss in Insomniac Rats

We further investigated the effects of right-sided SGB on neuronal loss in insomniac rats. HE staining showed that, compared to the Control group, rats in the Model group exhibited significant neuronal damage, including disrupted cellular architecture, nuclear shrinkage, cytoplasmic condensation with intense staining, and an increased intercellular gap. Notably, SGB treatment reduced brain tissue damage in the rats with insomnia (Fig. 2A, $p < 0.05$). Additionally, Nissl staining revealed a substantial decrease in Nissl body count in the Model group compared to the Control group, while the SGB group demonstrated a marked increase in Nissl bodies relative to the Sham group (Fig. 2B, $p < 0.05$). Immunohistochemistry analysis of presynap-

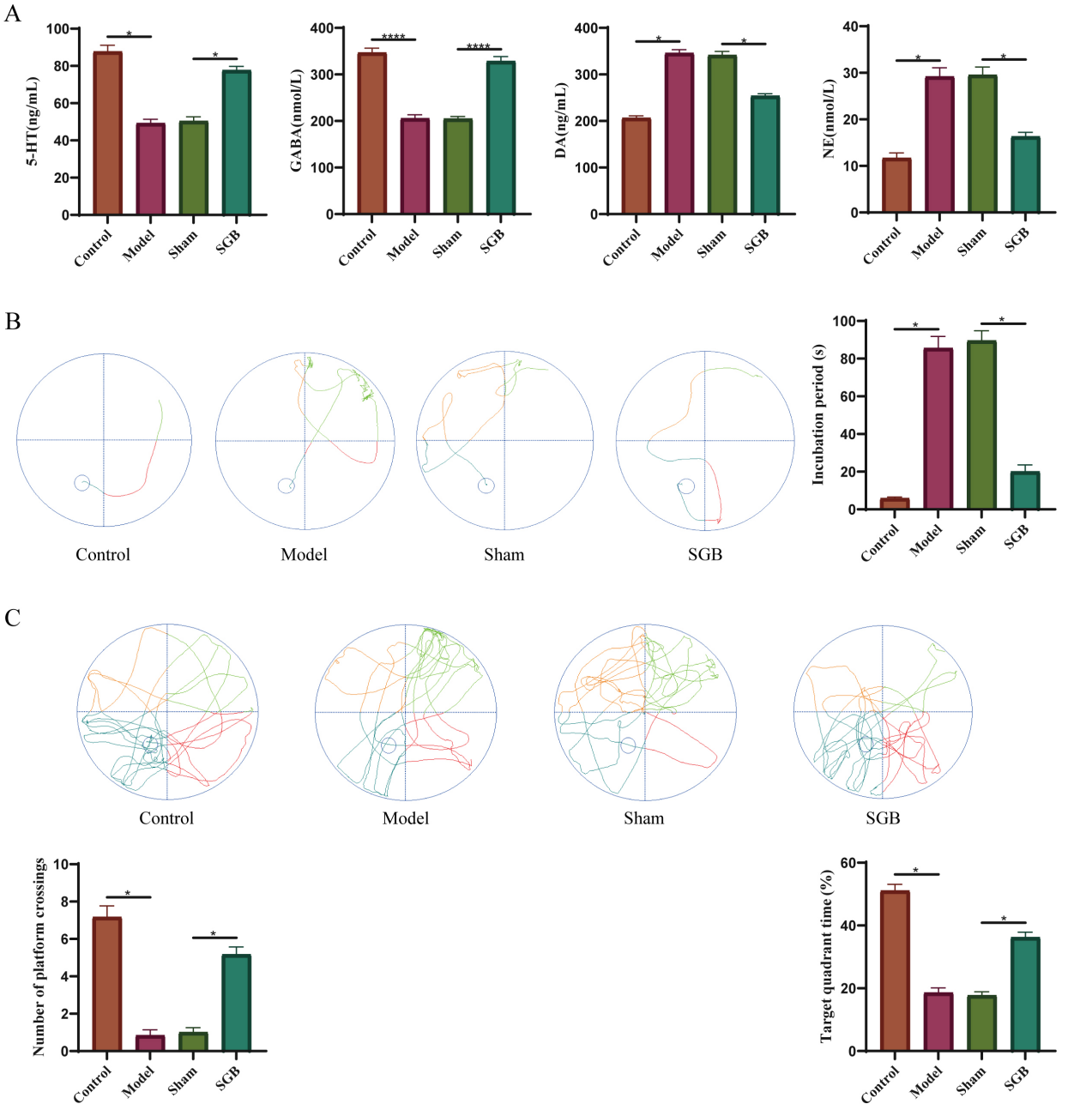

Fig. 1. Right-sided SGB improves cognitive impairment in insomniac rats. (A) Measurements of neurotransmitter levels (5-HT, GABA, DA, NE) using ELISA. (B) Assessment of the rats' navigation ability using the Morris water maze test. (C) Assessment of the rats' spatial exploration ability using the Morris water maze test. Data are presented as mean ± SD. Data analysis was performed using one-way ANOVA, *$p < 0.05$, ****$p < 0.0001$. $n = 6$. Abbreviations: DA, dopamine; GABA, γ-aminobutyric acid; 5-HT, serotonin; NE, noradrenaline; SGB, stellate ganglion block.

tic (synuclein (SYN)) and postsynaptic (PSD-95) markers in brain tissues showed that, compared to the Control group, the Model group had significantly reduced expression levels of both SYN and PSD-95. In contrast, the SGB group exhibited much higher expression of SYN and PSD-95 compared to the Sham group (Fig. 2C, $p < 0.05$). These findings indicate that right-sided SGB helps preserve synaptic integrity and reduce neuronal loss in rats with insomnia.

Right-sided SGB Mitigates Ferroptosis in Insomniac Rats

Previous studies have highlighted the role of ferroptosis in neurodegenerative diseases associated with cognitive impairments [21]. To explore the effects of right-sided SGB on ferroptosis in brain neurons of insomniac rats, we first assessed the expression of key iron metabolism-related proteins in brain tissues through Western blotting. The results revealed that, compared to the Control group, the insom-

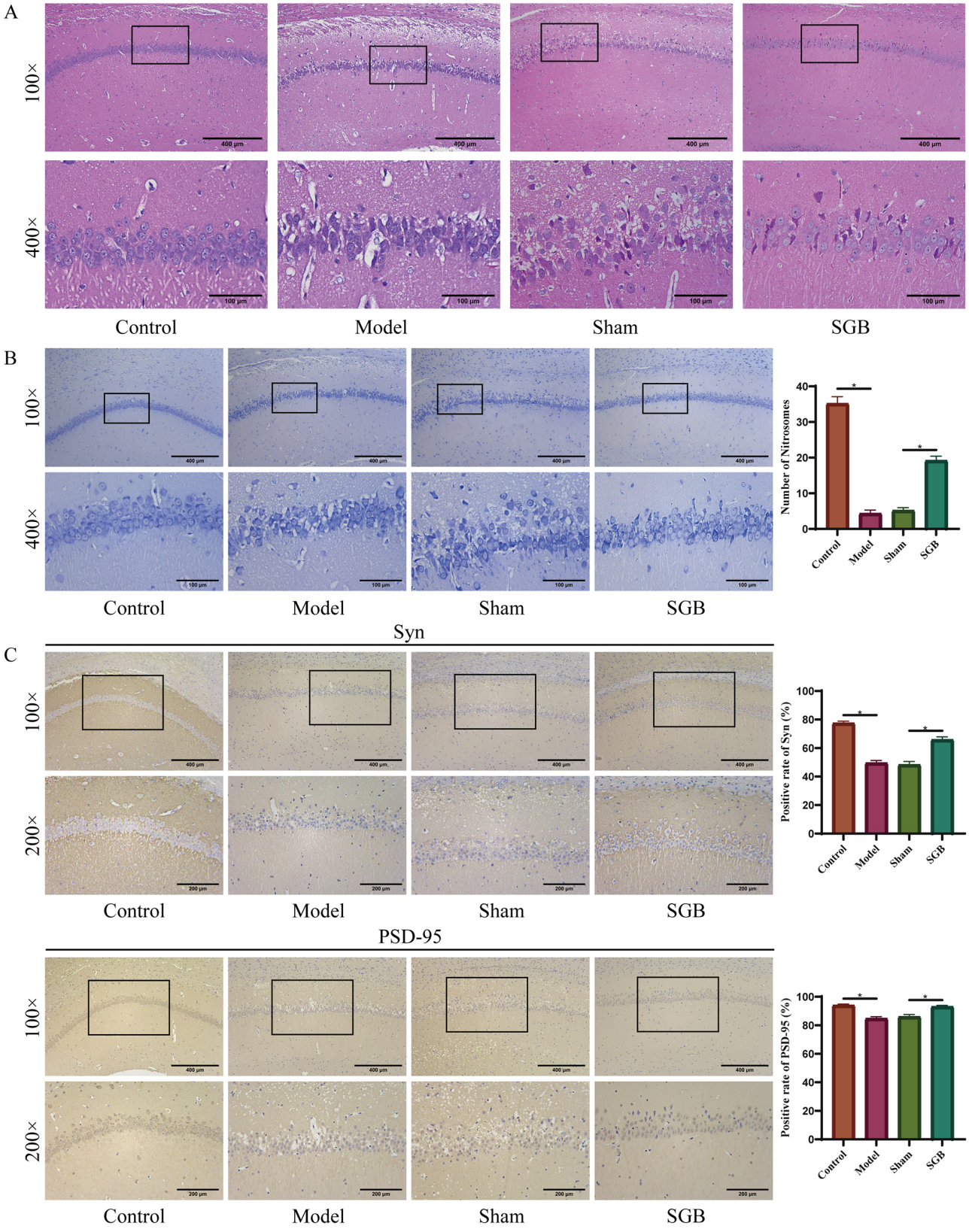

Fig. 2. Right-sided SGB improves neuronal loss in insomniac rats. (A) Assessment of brain tissue damage using HE staining. (B) Evaluation of Nissl bodies using Nissl staining and quantitative analysis. (C) Immunohistochemical staining of SYN and PSD-95, and quantitative analyses. Data are presented as mean ± SD. Data were analyzed using one-way ANOVA, *$p < 0.05$. $n = 6$. Abbreviation: PSD-95, postsynaptic density protein 95.

niac rats exhibited significantly higher expression levels of FTH1, FTL, and TFR1. However, in the SGB group, these proteins showed a significant reduction in expression relative to the Sham group (Fig. 3A, $p < 0.05$). We also measured iron concentrations in the brain tissues, and a notable increase was observed in iron levels in the insomniac rats compared to the Control group. Treatment with right-sided SGB, however, led to a marked reduction in iron content in the hippocampus of the insomniac rats (Fig. 3B, $p < 0.05$).

Lipid peroxidation is a hallmark of ferroptosis. ELISA analysis showed a significant rise in the lipid peroxidation marker MDA in insomniac rats compared to controls, while levels of the antioxidant GSH were significantly reduced. After right-sided SGB treatment, MDA levels decreased, and GSH levels were restored in the insomniac rats (Fig. 3B, $p < 0.05$). Furthermore, fluorescent staining revealed elevated ROS levels in the hippocampus of insomniac rats, relative to the Control group. However, right-sided SGB treatment significantly reduced ROS levels in the brain tissues of these rats (Fig. 3C, $p < 0.05$). These findings indicate that the right-sided SGB effectively mitigates ferroptosis in the brain tissues of rats suffering from insomnia.

Right-sided SGB Alleviates Neuroinflammation in Insomniac Rats by Inhibiting Ferroptosis

This study also explored the potential of right-sided SGB in reducing neuroinflammation in the brain tissues of insomniac rats through the inhibition of ferroptosis. To assess this, immunofluorescence staining (Fig. 4A) was used to measure the expression of the microglial marker IBA-1 and the astrocyte marker GFAP in brain tissues, while ELISA (Fig. 4B) was employed to quantify inflammatory cytokine levels in the serum, including TNF-α, IL-1β, and IL-6. The results showed that, compared to the Control group, the Model group exhibited significantly higher levels of IBA-1 and GFAP expression in the hippocampus, along with increased serum levels of TNF-α, IL-1β, and IL-6 ($p < 0.05$). In contrast, rats in the SGB group showed a significant reduction in both IBA-1 and GFAP expression in the brain tissue and lower serum concentrations of TNF-α, IL-1β, and IL-6 compared to the Sham group ($p < 0.05$). Further analysis revealed that, compared to the SGB group, rats treated with the ferroptosis inducer (RSL3) exhibited significantly increased IBA-1 and GFAP expression in the hippocampus, along with elevated serum levels of TNF-α, IL-1β, and IL-6 ($p < 0.05$). These findings suggest that right-sided SGB reduces neuroinflammation in the hippocampus of insomniac rats by inhibiting ferroptosis.

Right-sided SGB Inhibits Ferroptosis in Insomniac Rats via the NRF2/GPX4 Pathway

To explore the underlying mechanism by which right-sided SGB inhibits ferroptosis, we assessed key proteins in the NRF2/GPX4 pathway in the brain tissue of rats. The results showed a marked decrease in NRF2 and GPX4 protein levels in the hippocampus of the Model group versus the Control group. Conversely, SGB-treated rats exhibited markedly increased expression of these proteins compared to the Sham group ($p < 0.05$), indicating that right-sided SGB activates the NRF2/GPX4 pathway in the hippocampus of insomniac rats (Fig. 5A).

Next, we investigated how right-sided SGB influences ferroptosis in the brain tissue of insomniac rats through the NRF2/GPX4 pathway. Western blot analysis indicated that, compared to the SGB + NS group, inhibition of NRF2 by ML385 led to a significant upregulation of FTH1, FTL, and TFR1 in the hippocampus. However, when Fer-1 was administered, the levels of these proteins were considerably reduced (Fig. 5B, $p < 0.05$). Additionally, brain iron content increased significantly in the SGB + ML385 group versus the SGB + NS group, while the SGB + ML385 + Fer-1 group showed reduced iron accumulation (Fig. 5C, $p < 0.05$). Importantly, treatment with ML385 elevated ROS and MDA, and depleted GSH, whereas the administration of Fer-1 attenuated these changes (Fig. 5C,D, $p < 0.05$). To validate the role of NRF2 in SGB-mediated neuroprotection, we generated NRF2-knockdown rats. Knockdown of NRF2 reduced its hippocampal protein expression and elevated FTH1/FTL/TFR1 levels (Fig. 5E, $p < 0.05$). It also increased brain iron content and oxidative stress (increased MDA, decreased GSH) compared to controls (Fig. 5F, $p < 0.05$). These genetic and pharmacological interventions demonstrate that right-sided SGB inhibits ferroptosis in insomniac rats by activating the NRF2/GPX4 pathway, conferring neuroprotection.

Right-sided SGB Protects the Brain Tissue of Insomniac Rats From Damage via the NRF2/GPX4 Pathway

We further explored whether right-sided SGB protects brain tissue from damage in insomniac rats via the NRF2/GPX4 pathway. HE staining revealed that, after treatment with the NRF2 inhibitor ML385, the brain tissue exhibited significantly more damage than the SGB + NS group. However, this damage was notably reduced following subsequent treatment with Fer-1 (Fig. 6A, $p < 0.05$). Additionally, Nissl staining revealed that neuronal Nissl body counts markedly decreased in the SGB + ML385 group versus the SGB + NS group, but recovered significantly after Fer-1 treatment (Fig. 6B, $p < 0.05$). Immunohistochemistry further indicated that synaptic integrity was compromised in the SGB + ML385 group, showing reduced expression of presynaptic (SYN) and postsynaptic (PSD-95) markers. These deficits were reversed in the SGB + ML385 + Fer-1 group (Fig. 6C, $p < 0.05$). To genetically validate the role of NRF2, we conducted NRF2 knockdown. HE and Nissl staining showed severe neuronal damage in knockdown rats, manifesting as disorganized neuronal alignment and diminished Nissl bodies (Fig. 6D,E, $p < 0.05$). Immunohistochemical analysis confirmed sig-

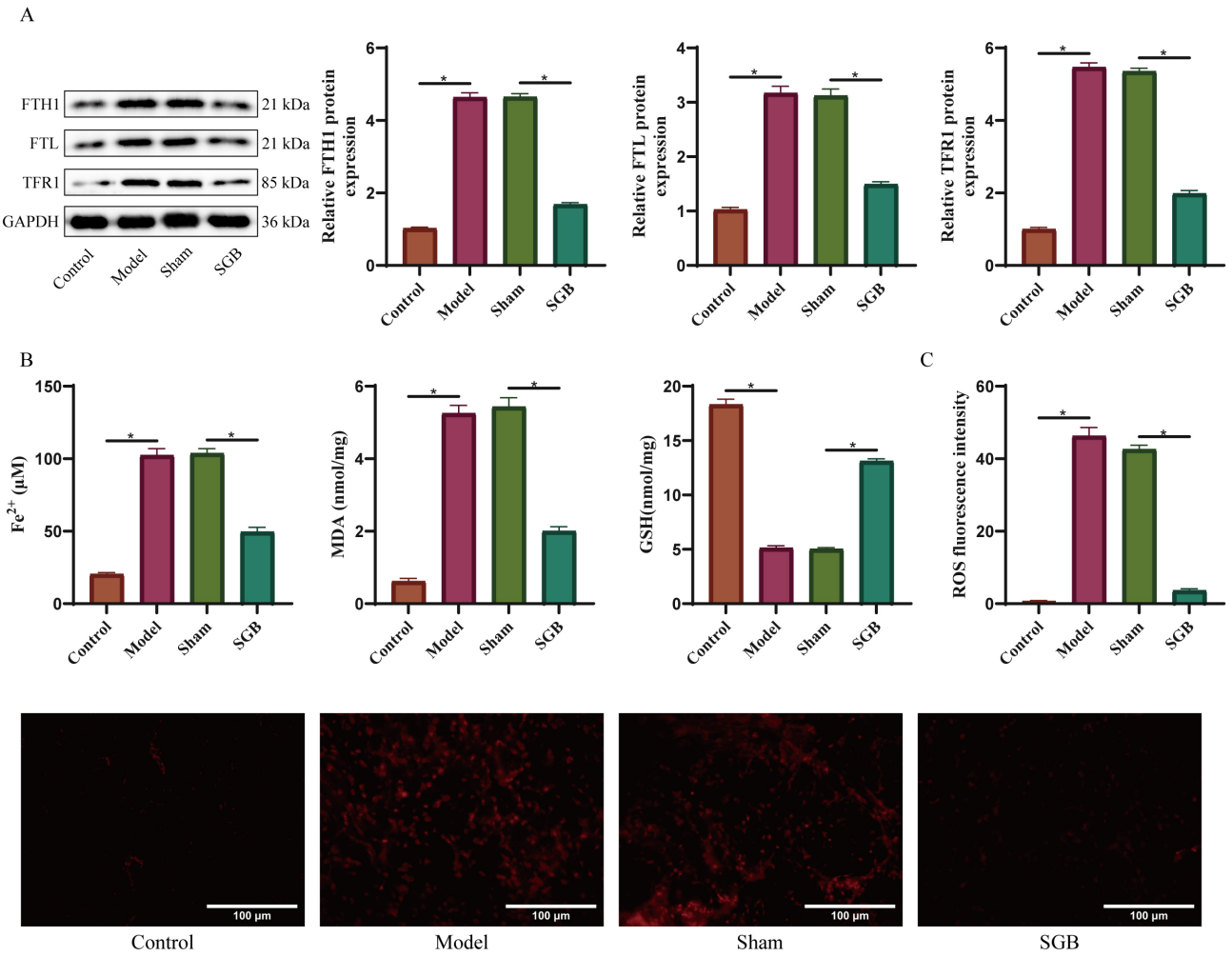

Fig. 3. Right-sided SGB mitigates ferroptosis in insomniac rats. (A) Expression levels of FTH1, FTL, and TFR1 were detected using Western blotting. (B) Measurements of ferrous ions, MDA and GSH levels using assay kits. (C) Detection of ROS levels by means of immunofluorescence staining. Data are presented as mean ± SD. Data were analyzed using one-way ANOVA, $*p < 0.05$. $n = 6$. Abbreviations: FTH1, ferritin heavy chain 1; FTL, ferritin light chain; GAPDH, glyceraldehyde-3-phosphate dehydrogenase; GSH, glutathione; MDA, malondialdehyde; ROS, reactive oxygen species; TFR1, transferrin receptor 1.

nificantly reduced SYN and PSD-95 expression (Fig. 6F, $p < 0.05$). These findings establish that SGB prevents neuronal damage and synaptic loss in insomnia by activating the NRF2/GPX4 pathway, offering direct proof that SGB exerts its neuroprotective effects through the NRF2 pathway. Right-sided SGB thus alleviates ferroptosis-mediated brain injury through NRF2-dependent mechanisms.

Discussion

Earlier research has highlighted the substantial impact of SGB in relieving neuropsychiatric disorders. For example, Capone *et al.* [22] reported that SGB notably alleviated symptoms in individuals with PTSD and enhanced their sleep quality. Additionally, Mulvaney *et al.* [23] found that in PTSD patients, SGB could modulate autonomic nervous system function, reducing sympathetic nervous system activity, thereby improving sleep. These studies support the potential of SGB to regulate the nervous system and improve insomnia. Consistent with these results, our research showed that SGB notably elevated the levels of inhibitory neurotransmitters (5-HT and GABA) in the brain tissue of insomniac rats, while reducing the concentrations of excitatory neurotransmitters (DA and NE), which aligns with SGB's sympatholytic nerve-blocking effects. The balance of neurotransmitters is crucial for maintaining normal neurological function, and conditions like insomnia are often associated with excessive release of excitatory neurotransmitters, which can lead to neuronal hyperexcitability and neurotoxicity [24]. By reducing sympathetic hyperactivity, SGB may rebalance the hypothalamic-pituitary-adrenal axis, mitigating neuronal hyperexcitability and oxidative stress, which is a plausible explanation for its neuroprotective effects [25]. Additionally, the Morris water maze test demonstrated that SGB notably alleviated cognitive deficits in insomniac rats, and HE staining and immunohistochem-

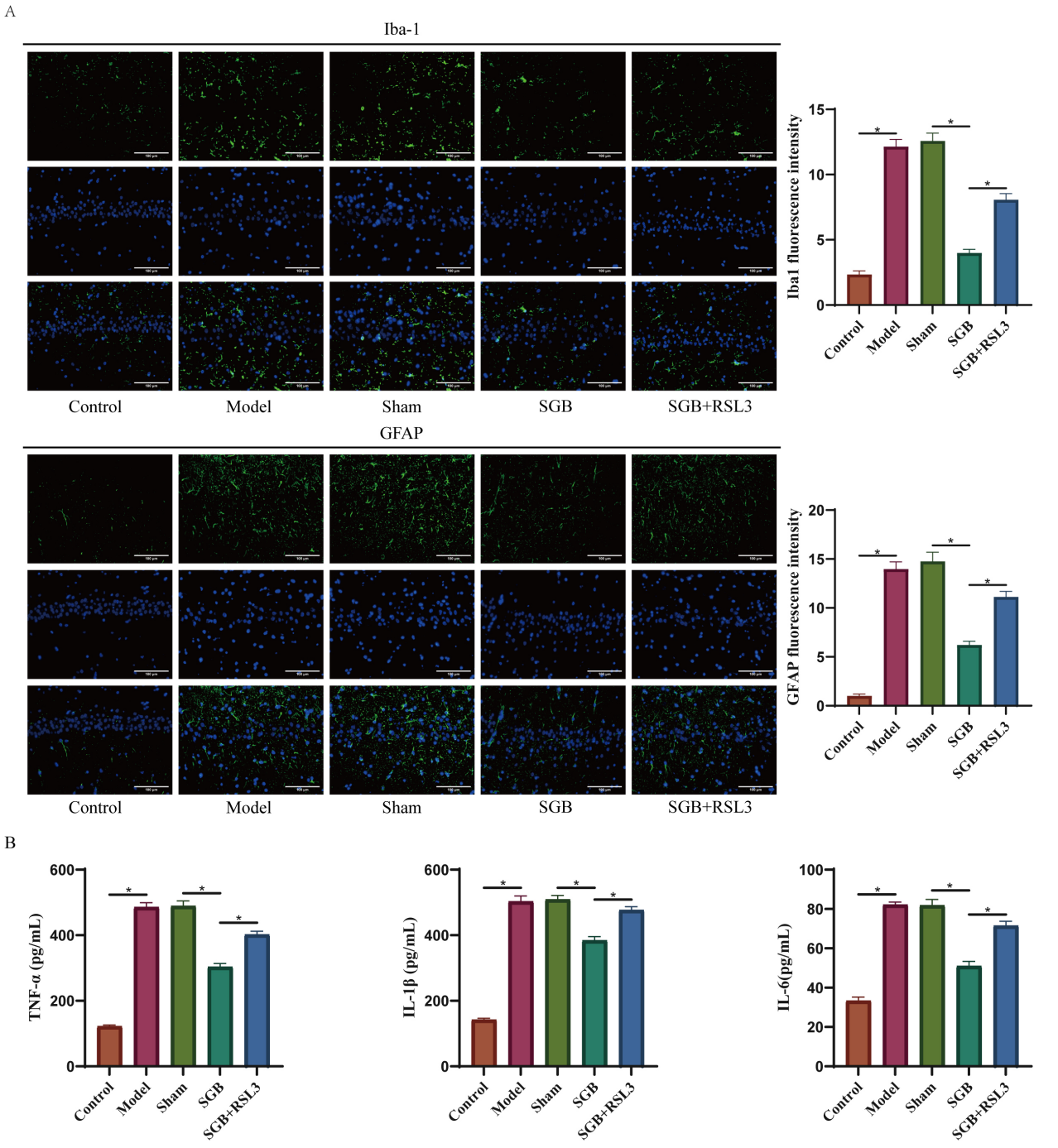

Fig. 4. Right-sided SGB alleviates neuroinflammation in insomniac rats by inhibiting ferroptosis. (A) Evaluation of IBA-1 and GFAP levels in rat brain tissues using immunofluorescence staining. (B) Detection of TNF-α, IL-1β, and IL-6 levels in rat serum by means of ELISA. Data are presented as mean $\pm$ SD. Data were analyzed using one-way ANOVA, *$p < 0.05$. $n = 6$. Abbreviations: GFAP, glial fibrillary acidic protein; IBA-1, ionized calcium-binding adaptor molecule 1; IL, interleukin; TNF-α, tumor necrosis factor alpha.

istry confirmed that SGB helped preserve synaptic integrity and minimize neuronal loss (indicated by SYN and PSD-95) in the brain tissue. While many studies have highlighted the potential of SGB in addressing insomnia, the precise mechanisms underlying its effects still need to be further explored.

Ferroptosis, a recently discovered type of cell death driven by iron and the buildup of lipid peroxides, is strongly associated with cognitive impairments in various neurological disorders [26]. This research is the first to investigate how SGB regulates ferroptosis in the brain tissue of rats with insomnia. The findings revealed that, in comparison to

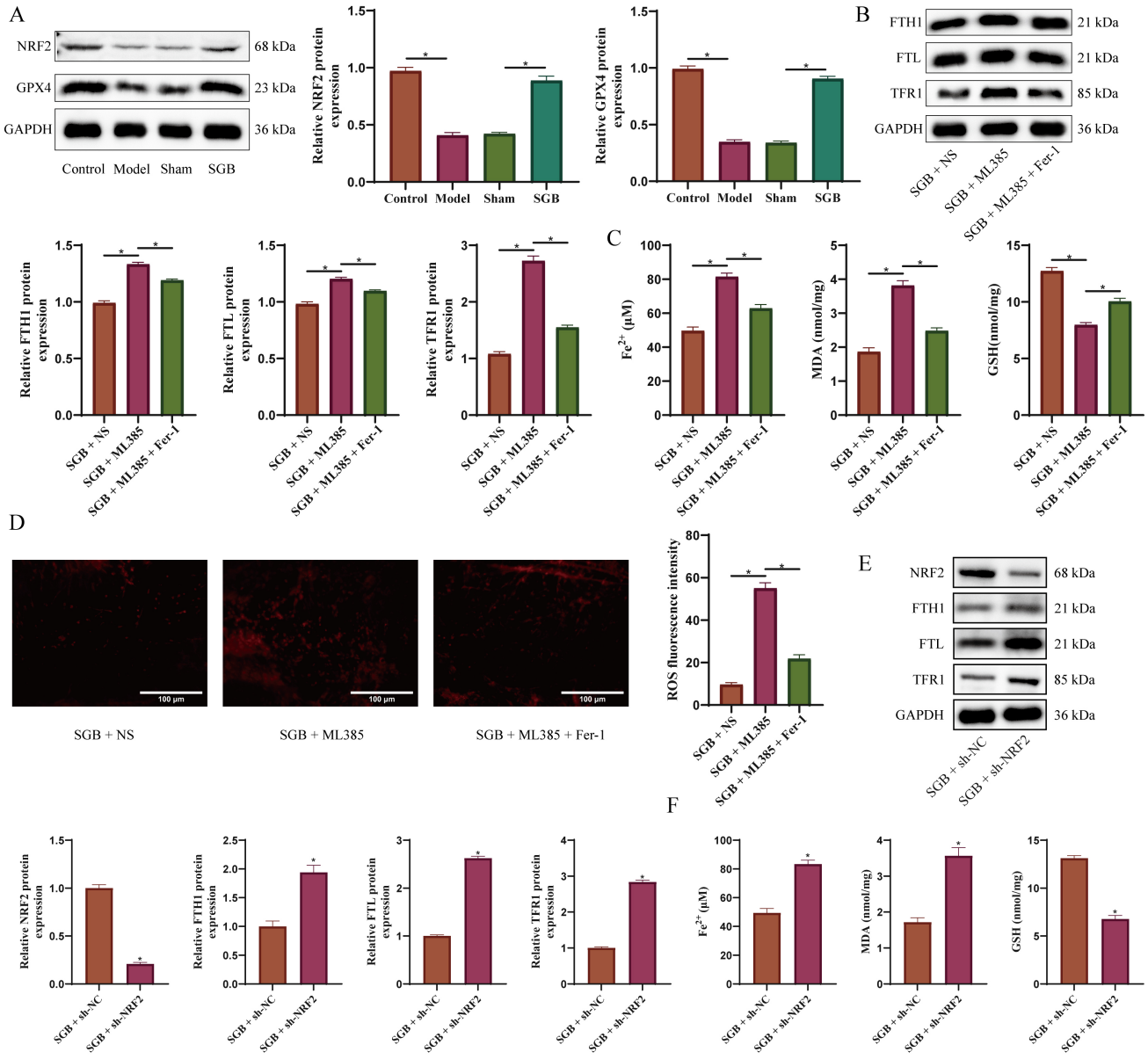

Fig. 5. Right-sided SGB inhibits ferroptosis in insomniac rats via the NRF2/GPX4 pathway. (A) Detection of NRF2 and GPX4 expression levels through Western blotting. (B) Detection of FTH1, FTL, and TFR1 expression levels through Western blotting. (C) Biochemical measurements of iron content, lipid peroxidation (MDA), and antioxidant capacity (GSH) in brain tissue after treatment with ML385 and/or Fer-1. (D) Detection of ROS levels by means of immunofluorescence staining. (E) Detection of NRF2, FTH1, FTL, and TFR1 expression levels. (F) Biochemical measurements of iron content, MDA, and GSH levels in NRF2-knockdown rats. Data are presented as mean ± SD. The *t*-test was employed for comparisons between two groups. Data were analyzed using one-way ANOVA, $*p < 0.05$. $n = 6$. Abbreviations: GPX4, glutathione peroxidase 4; NRF2, nuclear factor-erythroid 2-related factor 2.

the control group, the expression levels of proteins involved in iron metabolism (FTH1, FTL, and TFR1) were notably reduced, while iron content was substantially increased in the brain tissue of insomniac rats, which suggests impaired iron storage and transport, consistent with ferroptosis signatures in neurodegenerative disorders [21]. Treatment with SGB notably elevated the levels of proteins related to iron metabolism and decreased iron content, suggesting its potential to mitigate ferroptosis by correcting disturbances in iron metabolism. Moreover, SGB also decreased the level of lipid peroxide MDA and increased the level of the antioxidant GSH in the brain tissue of insomniac rats, further confirming its inhibitory effect on ferroptosis.

Neuroinflammation is one of the key pathological features of cognitive impairment associated with insomnia [27]. In this research, the impact of SGB on neuroinflammation in insomniac rats was assessed by measuring markers of microglial and astrocytic activation (IBA-1 and

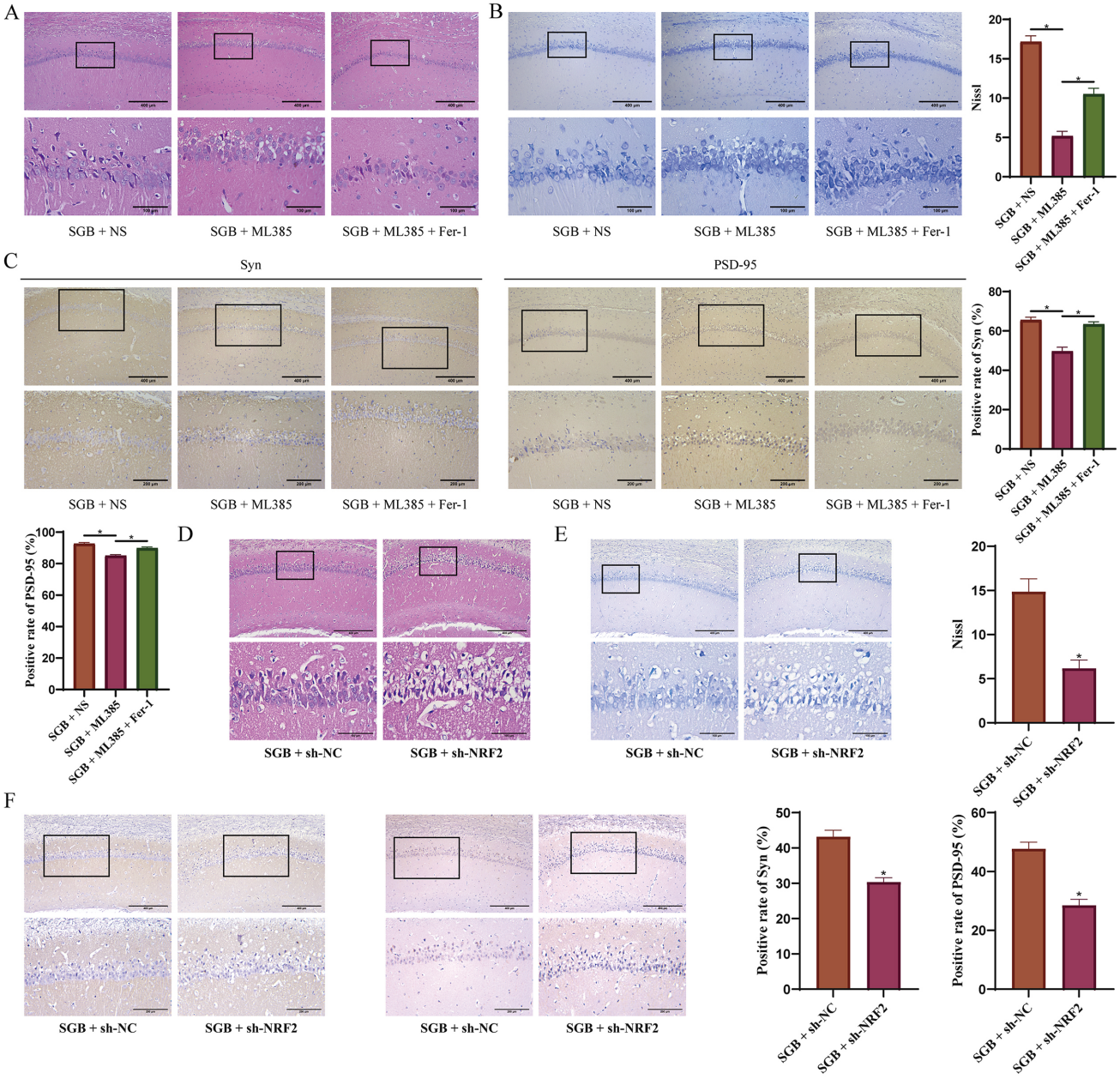

Fig. 6. Right-sided SGB protects the brain tissue of insomniac rats from damage via the NRF2/GPX4 pathway. (A) HE staining showing neuronal damage in hippocampal tissue after pharmacological treatments (SGB+NS, SGB+ML385, and SGB+ML385+Fer-1). (B) Nissl staining and quantitative analysis of Nissl bodies (right) in hippocampal neurons under different pharmacological conditions. (C) Immunohistochemical staining and quantification of presynaptic (SYN) and postsynaptic (PSD-95) protein expression following ML385 and Fer-1 treatment. (D) HE staining showing neuronal damage in the hippocampal tissue of NRF2-knockdown rats and controls. (E) Nissl staining and quantitative analysis of Nissl bodies in NRF2-knockdown rats. (F) Immunohistochemical staining and quantification of SYN and PSD-95 expression in NRF2-knockdown rats. Data are presented as mean ± SD. The *t*-test was employed for comparisons between two groups. Data were analyzed using one-way ANOVA, $*p < 0.05$. $n = 6$. Abbreviations: SYN, synuclein.

GFAP) in the brain tissue and by quantifying the levels of inflammatory cytokines in the serum. The findings indicated that SGB notably lowered the expression of IBA-1 and GFAP in the brain tissue of rats with insomnia, while also reducing the serum levels of inflammatory cytokines, highlighting its anti-neuroinflammatory properties. Moreover, the intervention with RSL3 counteracted the suppressive effect of SGB on inflammatory cytokines, implying that ferroptosis is a crucial factor in neuroinflammation. It is possible that SGB helps reduce the inflammatory response in insomniac rats by inhibiting ferroptosis.

Given the established role of the NRF2/GPX4 pathway in mediating antioxidative stress and regulating ferroptosis [4], we investigated its involvement in SGB-mediated

neuroprotection. Our analysis revealed significantly diminished NRF2 and GPX4 expression in the hippocampus of insomniac rats, while SGB significantly restored their protein levels, suggesting inhibition of ferroptosis via pathway activation. Pharmacological inhibition of NRF2 with ML385 abrogated this protective effect, confirming the pathway's essential contribution to SGB-mediated ferroptotic suppression. Critically, co-administration of Fer-1, a ferroptosis inhibitor, partially reversed ML385-induced neuronal and synaptic damage, further substantiating the central role of NRF2/GPX4-dependent ferroptosis suppression in SGB's neuroprotective mechanism.

While our preclinical findings are mechanistically compelling, clinical translation requires careful consideration of human physiological complexity and interindividual variability. Notably, the insomnia model used in this study, induced by acute serotonin depletion via PCPA, reflects primarily neurotransmitter dysregulation and may not fully replicate the chronicity, psychological stressors, and multifactorial etiology characteristic of human insomnia. Future preclinical studies should clarify additional molecular pathways modulated by SGB. Clinical research, particularly double-blind randomized controlled trials, should evaluate its safety, efficacy, and potential synergy with established insomnia treatments such as pharmacotherapy or cognitive-behavioral therapy. Although NRF2/GPX4 activation appears to alleviate hippocampal ferroptosis, the cell-type-specific contributions of astrocytes, microglia, and neurons remain unknown and warrant investigation using lineage-specific targeting approaches. Furthermore, as insomnia necessitates sustained management, potential risks associated with long-term or repeated SGB administration, including local tissue fibrosis, nerve injury, or anesthetic toxicity, should be prospectively assessed prior to clinical application.

Collectively, the findings of this study demonstrate that right-sided SGB significantly alleviates cognitive impairment and neuronal loss in PCPA-induced insomniac rats. Mechanistically, SGB activates the NRF2/GPX4 pathway, rectifies iron dyshomeostasis, reduces lipid peroxidation, and suppresses neuroinflammation, and these effects are dependent on ferroptosis inhibition. These results not only support the use of SGB as a potential non-pharmacological intervention for insomnia-related neurodegeneration but also present a novel approach to understanding the underlying pathological mechanisms of the condition.

Conclusion

In conclusion, our findings demonstrate that right-sided SGB exerts multifaceted neuroprotective effects in a PCPA-induced insomnia model. Mechanistically, SGB activates NRF2/GPX4 signaling to suppress ferroptosis by restoring iron homeostasis, attenuating lipid peroxidation, and mitigating neuroinflammation. These coordinated actions preserve synaptic integrity, reduce neuronal loss, and ultimately rescue cognitive deficits in insomniac rats. Our study not only elucidates the critical role of ferroptosis in insomnia-related neurodegeneration but also positions right-sided SGB as a novel neuromodulatory intervention with translational potential. Future clinical studies should validate these findings in human populations and explore synergistic strategies combining SGB with existing therapies to optimize outcomes in insomnia management.

Availability of Data and Materials

The data used and analyzed during the current study are available from the corresponding author.

Author Contributions

MYL: Conceptualization; Visualization. XOY: Data Curation; Validation. YS: Investigation; Methodology. QZ: Formal Analysis; Software; Writing – Original Draft Preparation. All authors were involved in critical revision of the manuscript. All authors have read and approved the final manuscript. All authors have participated sufficiently in the work and agreed to be accountable for all aspects of the work.

Ethics Approval and Consent to Participate

All experimental procedures were conducted in strict accordance with the 3Rs principles (Replacement, Reduction, Refinement) and approved by the Animal Ethics Committee of Hunan Evidence-based Biotechnology Co., Ltd. (Approval No. ABZH24001).

Acknowledgment

Not applicable.

Funding

This research is supported by Shanghai Jing'an District Science and Technology Commission General Project (Grant No. 2022MS06).

Conflict of Interest

The authors declare no conflict of interest.

References

[1] Riemann D, Benz F, Dressle RJ, Espie CA, Johann AF, Blanken TF, *et al*. Insomnia disorder: State of the science and challenges for the future. Journal of Sleep Research. 2022; 31: e13604. https://doi.org/10.1111/jsr.13604.

[2] Dopheide JA. Insomnia overview: epidemiology, pathophysiology, diagnosis and monitoring, and nonpharmacologic therapy.

The American Journal of Managed Care. 2020; 26: S76–S84. https://doi.org/10.37765/ajmc.2020.42769.

[3] Simon L, Terhorst Y, Cohrdes C, Pryss R, Steinmetz L, Elhai JD, *et al*. The predictive value of supervised machine learning models for insomnia symptoms through smartphone usage behavior. Sleep Medicine: X. 2024; 7: 100114. https://doi.org/10.1016/j.sleepx.2024.100114.

[4] Javaheri S, Redline S. Insomnia and Risk of Cardiovascular Disease. Chest. 2017; 152: 435–444. https://doi.org/10.1016/j.chest.2017.01.026.

[5] Maheshwari V, Basu S. Sleep problems and their predictors in community-dwelling older adults with diabetes in India: Evidence from the Longitudinal Ageing Study in India. Sleep Medicine: X. 2024; 7: 100108. https://doi.org/10.1016/j.sleepx.2024.100108.

[6] Ma Y, Yu S, Li Q, Zhang H, Zeng R, Luo R, *et al*. Sleep patterns, genetic susceptibility, and digestive diseases: a large-scale longitudinal cohort study. International Journal of Surgery (London, England). 2024; 110: 5471–5482. https://doi.org/10.1097/JS9.0000000000001695.

[7] Hua Y, Guo S, Xie H, Zhu Y, Yan H, Tao WW, *et al*. *Ziziphus jujuba* Mill. var. *spinosa* (Bunge) Hu ex H. F. Chou Seed Ameliorates Insomnia in Rats by Regulating Metabolomics and Intestinal Flora Composition. Frontiers in Pharmacology. 2021; 12: 653767. https://doi.org/10.3389/fphar.2021.653767.

[8] Rajendran PS, Hanna P. The irate stellate ganglion: IL-6 in neuroinflammation-induced ventricular arrhythmias. Heart Rhythm. 2024; 21: 620–621. https://doi.org/10.1016/j.hrthm.2024.01.030.

[9] Ryu H, Kim H. The usefulness of stellate ganglion block with ultrasound-guided lateral paracarotid approach in ventricular arrhythmias: A case series. Saudi Journal of Anaesthesia. 2024; 18: 276–279. https://doi.org/10.4103/sja.sja_657_23.

[10] Zhao Y, Xiao X. Efficacy of ultrasound-guided stellate ganglion block in relieving acute postoperative pain: a systematic review and meta-analysis. The Journal of International Medical Research. 2024; 52: 3000605241252237. https://doi.org/10.1177/03000605241252237.

[11] Lu DH, Xu XX, Zhou R, Wang C, Lan LT, Yang XY, *et al*. Ultrasound-guided stellate ganglion block benefits the postoperative recovery of patients undergoing laparoscopic colorectal surgery: a single-center, double-blinded, randomized controlled clinical trial. BMC Anesthesiology. 2024; 24: 137. https://doi.org/10.1186/s12871-024-02518-5.

[12] Jiang X, Stockwell BR, Conrad M. Ferroptosis: mechanisms, biology and role in disease. Nature Reviews. Molecular Cell Biology. 2021; 22: 266–282. https://doi.org/10.1038/s41580-020-00324-8.

[13] Ye X, Wang W, Zheng Y, Han X. Preliminary research on the role of ferroptosis in insomnia. Asian Journal of Surgery. 2024; S1015–S1015–9584(24)02182–1. https://doi.org/10.1016/j.asjsur.2024.09.137. (online ahead of print)

[14] Dodson M, Castro-Portuguez R, Zhang DD. NRF2 plays a critical role in mitigating lipid peroxidation and ferroptosis. Redox Biology. 2019; 23: 101107. https://doi.org/10.1016/j.redox.2019.101107.

[15] Yuan Y, Zhai Y, Chen J, Xu X, Wang H. Kaempferol Ameliorates Oxygen-Glucose Deprivation/Reoxygenation-Induced Neuronal Ferroptosis by Activating Nrf2/SLC7A11/GPX4 Axis. Biomolecules. 2021; 11: 923. https://doi.org/10.3390/biom11070923.

[16] Liu Y, Wan Y, Jiang Y, Zhang L, Cheng W. GPX4: The hub of lipid oxidation, ferroptosis, disease and treatment. Biochimica et Biophysica Acta. Reviews on Cancer. 2023; 1878: 188890. https://doi.org/10.1016/j.bbcan.2023.188890.

[17] Gurrea-Rubio M, Wang Q, Mills EA, Wu Q, Pitt D, Tsou PS, *et al*. Siponimod Attenuates Neuronal Cell Death Triggered by Neuroinflammation via NFκB and Mitochondrial Pathways. International Journal of Molecular Sciences. 2024; 25: 2454. https://doi.org/10.3390/ijms25052454.

[18] Chen Y, Fang ZM, Yi X, Wei X, Jiang DS. The interaction between ferroptosis and inflammatory signaling pathways. Cell Death & Disease. 2023; 14: 205. https://doi.org/10.1038/s41419-023-05716-0.

[19] Wang Z, Li D, Chen M, Yu X, Chen C, Chen Y, *et al*. A comprehensive study on the regulation of Compound Zaoren Granules on cAMP/CREB signaling pathway and metabolic disorder in CUMS-PCPA induced insomnia rats. Journal of Ethnopharmacology. 2024; 332: 118401. https://doi.org/10.1016/j.jep.2024.118401.

[20] Shi ZM, Jing JJ, Xue ZJ, Chen WJ, Tang YB, Chen DJ, *et al*. Stellate ganglion block ameliorated central post-stroke pain with comorbid anxiety and depression through inhibiting HIF-1α/NLRP3 signaling following thalamic hemorrhagic stroke. Journal of Neuroinflammation. 2023; 20: 82. https://doi.org/10.1186/s12974-023-02765-2.

[21] Xue C, He Z, Zeng M, Wang Z, Chen Q, Qin F, *et al*. The Protective Effects of *Polygala tenuifolia* and Tenuifolin on Corticosterone-Evoked Ferroptosis, Oxidative Stress, and Neuroinflammation: Insights from Molecular Dynamics Simulations and In Vitro Experiments. Foods (Basel, Switzerland). 2024; 13: 3358. https://doi.org/10.3390/foods13213358.

[22] Capone C, Eaton E, Shea MT, Borgia M, DeMoss L, Tocco K, *et al*. A pilot study of stellate ganglion block paired with exposure therapy: Feasibility and acceptability in combat veterans with posttraumatic stress disorder. Psychological Trauma: Theory, Research, Practice and Policy. 2024; 10.1037/tra0001679. https://doi.org/10.1037/tra0001679. (online ahead of print)

[23] Mulvaney SW, Lynch JH, Hickey MJ, Rahman-Rawlins T, Schroeder M, Kane S, *et al*. Stellate ganglion block used to treat symptoms associated with combat-related post-traumatic stress disorder: a case series of 166 patients. Military Medicine. 2014; 179: 1133–1140. https://doi.org/10.7205/MILMED-D-14-00151.

[24] Liu H, Yang L, Wan C, Li Z, Yan G, Han Y, *et al*. Evaluation of the pharmacological effects and exploration of the mechanism of traditional Chinese medicine preparation Ciwujia tablets in treating insomnia based on ethology, energy metabolism, and urine metabolomic approaches. Frontiers in Pharmacology. 2022; 13: 1009668. https://doi.org/10.3389/fphar.2022.1009668.

[25] Lipov E, Kelzenberg B, Rothfeld C, Abdi S. Modulation of NGF by cortisol and the Stellate Ganglion Block - is this the missing link between memory consolidation and PTSD? Medical Hypotheses. 2012; 79: 750–753. https://doi.org/10.1016/j.mehy.2012.08.019.

[26] Bao WD, Pang P, Zhou XT, Hu F, Xiong W, Chen K, *et al*. Loss of ferroportin induces memory impairment by promoting ferroptosis in Alzheimer's disease. Cell Death and Differentiation. 2021; 28: 1548–1562. https://doi.org/10.1038/s41418-020-00685-9.

[27] Wang Y, Shan Z, Zhang L, Fan S, Zhou Y, Hu L, *et al*. P2X7R/NLRP3 signaling pathway-mediated pyroptosis and neuroinflammation contributed to cognitive impairment in a mouse model of migraine. The Journal of Headache and Pain. 2022; 23: 75. https://doi.org/10.1186/s10194-022-01442-8.